Supplementary Materials

Vaccine-Elicited CD4 T Cells Induce Immunopathology Following Chronic LCMV Infection

Pablo Penaloza-MacMaster[1], Daniel L. Barber[2], E. John Wherry[3], Nicholas M. Provine[1], Jeffrey E. Teigler[1], Lily Parenteau[1], Stephen Blackmore[1], Erica N. Borducchi[1], Rafael A. Larocca[1], Kathleen B. Yates[4], Hao Shen[3], W. Nicholas Haining[4], Rami Sommerstein[5], Daniel D. Pinschewer[5,6], Rafi Ahmed[7], Dan. H. Barouch[1, 8,*]

[1]Center for Virology and Vaccine Research, Beth Israel Deaconess Medical Center, Boston, MA 02215, USA. [2]Laboratory of Parasitic Diseases, National Institute of Allergy and Infectious Diseases, National Institutes of Health, Bethesda MD 20892, USA. [3]Department of Microbiology and Institute for Immunology, Perelman School of Medicine, University of Pennsylvania, Philadelphia, PA 19104, USA. [4]Department of Pediatric Oncology, Dana-Farber Cancer Institute, Harvard Medical School, Boston, MA 02115. [5]Department of Pathology and Immunology & W.H.O. Collaborating Centre for Vaccine Immunology, University of Geneva, 1211 Geneva, Switzerland. [6]Department of Biomedicine – Haus Petersplatz, Division of Experimental Virology, University of Basel, 4009 Basel, Switzerland. [7]Emory Vaccine Center and Department of Microbiology and Immunology, Emory University School of Medicine, Atlanta, GA 30322, USA. [8]Ragon Institute of MGH, MIT, and Harvard, Boston, MA 02114.

This PDF file includes:

Figures S1 to S13
Tables S1 to S3

Materials and Methods

Mice and Infections:

6-8 week old C57BL/6 mice (Jackson) were immunized with $3x10^4$ CFU and boosted homologously at day 60 with 10^6 CFU of a *Listeria monocytogenes* vaccine expressing a single CD4 T cell epitope derived from LCMV GP61-80 (LMgp61)(*14*). Immunizations were performed intravenously (i.v.). After 30 days, LMgp61 immune mice were challenged i.v. with $2x10^6$ PFU of LCMV Cl-13 (resulting in a persistent infection), as described previously or intraperitoneally (i.p.) with $2x10^5$ PFU of LCMV Armstrong (resulting in an acutely controlled infection)(*30*). To assess the role of virus-specific antibody responses at preventing immune dysregulation by memory CD4 T cells, we challenged mice with a genetically engineered LCMV Cl-13 (rCl-13/WE-GP) expressing the GP of the WE strain instead of its own GP and administered 500 μg of anti-WE GP antibody i.p. (clone KL25) on days -1 and 0 of infection. rCl-13/WE-GP and an analogous virus lacking amino acids 61-68 of WE-GP (rCl-13WE-GPΔgp61), a deletion known to be viable(*31*), were generated by reverse genetic techniques as previously described(*32*).

Peptide-pulsed dendritic cell (DC) vaccinations were performed as previously described(*33*). In brief, bone marrow derived DCs were in vitro expanded for 5 days with GM-CSF, and were then matured for 1 day with LPS, and coated with the

indicated MHC-II restricted peptides for 2 hr. Cells were extensively washed prior to injection. C57BL/6 mice received $4x10^5$ peptide-coated DCs and after one week, they received $20x10^7$ peptide coated spleen cells. After 50 days, mice were boosted with $1.4x10^6$ peptide coated DCs, and challenged with LCMV Cl-13 at day 40 post-boost. For BALB/c experiments, a single DC prime was performed, and mice were challenged with LCMV Cl-13 after three weeks following immunization. All DC vaccinations were done i.v. The complete sequences of all the various CD4 epitopes that were used are as follows: GP61 (GP61-80) GLNGPDIYKGVYQFKSVEFD; GP6 (GP6-20) TMFEALPHIIDEVIN; GP126 (GP126-140) TSAFNKKTFDHTLMS; NP309 (NP309-328): SGEGWPYIACRTSIVGRAWE; NP116 (NP116-130) SERPQASGVYMGNLT.

For experiments where viral control was assessed, $2x10^6$ PFU of LCMV (either Cl-13 or Armstrong) were given i.v. Titration of LCMV was performed on Vero cell monolayers as described previously(*34*). LCMV-specific IgG responses were detected by standard ELISA using lysates of BHK-21 cells infected with LCMV Cl-13. H-$2K^b$ deficient mice (Taconic) were utilized to avoid the generation of memory H-$2K^b$ restricted GP70-specific CD8 T cell responses. All mouse experiments were performed with approval by the BIDMC Institutional Animal Care and Use Committee (IACUC).

Histology:

Following euthanasia, mouse carcasses were placed in Bouin's fixative (Polysciences, Inc), and whole mouse necropsy and H&E stains were performed at the Dana Farber Mouse Histopathology Core (220 Longwood Ave, Boston MA 02115).

Cell depletions and cell transfers:

CD4 T cell depletions were performed by i.p. injection of 500 μg of GK1.5 antibody (BioXcell) given for two consecutive days before Cl-13 challenge. CD8 T cell depletions were performed by i.p. injection of 500 μg of 2.43 antibody (BioXcell) given 4 weeks before to Cl-13 challenge to remove LCMV-specific CD8 T cell responses generated by LMgp33 or VVgp33 immunization. Rat IgG2b (BioXcell) was used as negative control. For adoptive transfers, 10^6 P14 cells or LCMV Armstrong-immune CD8 T cells (day 45 post-infection) were injected i.v. one day before LCMV Cl-13 challenge.

Reagents and flow cytometry:

Single cell suspensions were obtained from blood and tissues as previously described (*35*). Intracellular cytokine staining was performed after surface staining followed by fixation and permeabilization (cytofix/cytoperm, Perm Wash; BD Biosciences). Intracellular staining of Foxp3 was performed according to manufacturer's instructions (eBioscience). Dead cells were excluded by gating out cells positive for Live/Dead fixable dead cell stain (Invitrogen). LCMV MHC class I and class II tetramers were obtained from the NIH tetramer facility (Emory

University). I-Ab GP66 tetramer was used to detect LCMV-specific CD4 T cells. Samples were acquired with a Becton Dickinson LSRII and analyzed using FlowJo (Treestar).

Microarray Data Acquisition and Analysis:

Gene expression profiling was performed as previously described(*36, 37*) and data were uplodaded (GSE number GSE63825). Briefly, LCMV-specific $CD4^+$ T cells were sorted to ≥98% purity on a FACS Aria (BD Biosciences) using I-Ab GP66 tetramers (which recognize the core GP61-80 CD4 epitope sequence) as previously shown(*27*). Sorted cells were stored at -80°C in 1ml of TRIzol (Life Sciences). RNA extraction was performed using the RNAdvance Tissue Isolation kit (Agencourt) as per manufacturer's instructions. The cDNA synthesis was performed using the Ovation Pico WTA v2 kit (NuGEN) following manufacturer's instructions. Proper amplification of cDNA was confirmed using an Agilent 2100 Bioanalyzer (Agilent Technologies) and performed by the Harvard Biopolymers Facility. cDNA was subsequently fragmented and biotinylated using an Encore Biotin Module 4200 (NuGEN). cDNA was hybridized to Mouse Genome 430 v2.0 chip (Affymetrix) by the Microarray Core of Dana Farber Cancer Institute. RMA method was used to process data image files. Differential gene expression was determined using GENE-E v3.0.163 (Broad Institute). Probes were collapsed to genes and $\log_2$ corrected. Gene set enrichment analysis and leading edge analysis were performed using GSEA v2.0.12 (Broad Institute). The following gene set collections were used: C2 v4.0, C5 v4.0, and C7 v4.0 (http://www.broadinstitute.org/gsea/msigdb/index.jsp). CD4 T

cell signatures were from published data sets: CD4 T cell exhaustion and memory(*27*), Th1, Th2, Th17, iTreg, and naïve(*38*), Tfh(*39*), and anergic T cells(*40*). Permutation was performed on gene set. Gene ontology terms were determined using GOrilla http://cbl-gorilla.cs.technion.ac.il(*41, 42*). Genes within each cluster were compared against the complete list of genes in the dataset.

Statistical analysis:

Statistical analyses for survival plots were done using the Mantel-Cox test. All other analyses were performed using the Mann Whitney test. Data were analyzed using Prism (Graphpad).

Fig. S1. GP61-specific CD4 T cell responses following LM-GP61 immunization. A) Representative FACS plots showing GP61-80-specific CD4 T cell responses in blood following immunization with LM-GP61. B) Summary of GP61-specific CD4 T cell responses in blood following immunization with LM-GP61. Data are from 2 experiments, n=4 mice/group per experiment. Error bars indicate SEM.

Fig. S2. Vaccine-induced CD4 T cell immunopathology also occurs with different immunization regimens, different epitopes, and different mouse strains. A) Experimental outline for assessing the role of other memory CD4 T cell responses in C57BL/6 mice. B) Percent survival in C57BL/6 mice vaccinated with other CD4 T cell epitopes. C) Experimental outline for assessing the role of other memory CD4 T cell responses in BALB/c mice. D) Percent survival in BALB/c mice vaccinated with a nucleoprotein-specific CD4 T cell epitope. Statistical analyses for survival plots were performed using the Mantel-Cox test. Panels B and D are from 2 experiments, N=4-5 mice/group per experiment.

Fig. S3. Overall gating scheme for enumeration for virus-specific immune responses. A) Gating scheme for I-A^{b}GP66+ CD4 T cells. In order to reduce staining background, CD8 T cells (CD8+), B cells (B220+) and macrophages (F4/80+) were excluded. A side-by-side comparison was performed using I-A^{b}CLIP as negative control stain. B) Gating scheme for germinal center B cells. C) Gating scheme for H-2D^{b}GP276+ and H-2D^{b}GP33+ CD8 T cell responses.

Fig. S4. Similar pattern of viral tropism following LM-GP61 vaccination and chronic viral challenge. A) Viral loads in tissues. B) Representative FACS plots showing viral antigen in different cell subsets. C) Summary of viral antigen expression in different cell subsets. *, P=0.05; **, P= 0.03; **, P=0.01 (Mann-Whitney test). Data are from spleen on day 8.5, and from 2 experiments, n=4 mice/group per experiment. Error bars indicate SEM.

Fig. S5. Overall CD4 T cell and Treg collapse in LMgp61 vaccinated mice following LCMV Cl-13 challenge. A) Representative FACS plot of systemic CD4 and Treg responses. B) Numbers of CD4 T cells C) Numbers of Tregs. D) Effector (gp61-specific) to Treg ratio. E) Numbers of lymphocytes per mL of blood. Data are from PBMCs on day 8.5, and from 3 experiments, n=3-4 mice/group per experiment. *, P=0.05; **, P=0.03; ***, P=0.003 (Mann-Whitney test). Error bars indicate SEM.

Fig. S6. Increase in the precursor frequency of virus-specific CD4 T cells impairs antiviral immunity following LCMV Cl-13 challenge. A) Experimental outline. B) Percent survival. C) Longitudinal analysis of LCMV-specific IgG responses in sera. D) Longitudinal analysis of viral control in sera. Statistical analyses for survival plots were performed using the Mantel-Cox test. All other analyses were performed using the Mann-Whitney test. Data are from 2 experiments, N=5-7 mice/group per experiment. *, P=0.05; **, P=0.02; ***, P=0.007. Error bars indicate SEM.

Fig. S7. The subdominant GP70-77 CD8 T cell epitope is embedded in the GP61-80 CD4 T cell epitope. There is a H-2K^b-restricted subdominant CD8 T cell epitope nested within the GP61-80 CD4 T cell epitope. A) Amino acid sequence of the H-2K^b-restricted GP70-77 epitope. B) LM-GP61 vaccination primes the H-2K^{b}GP70-77 specific CD8 T cell response. H-2K^{b}GP70-77 specific CD8 T cells were measured at day 30 of LM-wt or LM-GP61 immunization. Data were corroborated in 3 experiments. N=4 mice/group per experiment.

Fig. S8. Immunopathogenesis of the LM-GP61 vaccine in H-2K^b deficient mice following LCMV Cl-13 challenge. At day 30 post-vaccination, mice were challenged with LCMV Cl-13. A) Weight loss. B) Percent survival. Data are from 2 experiments, n=4-5 mice/group.

Fig. S9. Phenotypic characterization of CD4 T cell dysregulation. A) Representative FACS plot showing that splenic I-Ab GP66+ CD4 T cells do not differentiate into FoxP3+ Tregs (gated from total CD4 T cells). B) Representative FACS plots showing similar Tfh conversion between LM-wt and LM-GP61 vaccinated mice. C) Decreased Eomes expression by dysregulated CD4 T cells. D) Increased CCR5 expression by dysregulated CD4 T cells. Data from panels B, C and D are gated from I-Ab GP66+ CD4 T cells (gating scheme on Fig. S3A). All data are from day 9 following LCMV Cl-13 challenge. Data are from 2 experiments, n=4 mice/group per experiment. *, P=0.02; **, P=0.0002 (Mann-Whitney test). Error bars indicate SEM.

Fig. S10. Functional characterization of CD4 T cell dysregulation. A) Representative FACS plot showing similar T helper differentiation patterns between LM-wt and LM-GP61 vaccinated groups. Note the typical Th1 differentiation (IFNγ, TNFα, IL-2) with partial Tfh differentiation (IL-21). Splenocytes were stimulated for 5 hr at 37°C with GP61 peptide, and stained with the indicated antibodies. IL-21 staining was performed with IL-21R-Fc. All data are from day 9 following LCMV Cl-13 challenge. Data are representative of 2 experiments, n=4 mice/group per experiment.

Fig. S11. Hierarchical clustering of leading edge analysis for all gene sets enriched in LMgp61 with a p value <0.01. Enriched gene sets are rows and enriched genes are columns. Yellow boxes denote when a specific gene is enriched in a specific gene set. Gene ontology terms were determined using GOrilla (http://cbl-gorilla.cs.technion.ac.il/). Data are based on cDNA microarray analysis of Figure 4.

Fig. S12. GP61-specific CD4 T cells provide help to adaptive immune responses following an acutely controlled LCMV Armstrong challenge. A) Experimental outline. B) Representative FACS plot showing splenic I-Ab GP66+ CD4 T cells following acute LCMV Armstrong challenge (day 8). C) Numbers of I-Ab GP66-specific CD4 T cells in spleen following acute LCMV Armstrong challenge (day 8). D) Magnitudes of LCMV-specific (DbGP276+) CD8 T cells. E) Percent expression of CD62L on LCMV-specific CD8 T cells. F) Expression of CD127. G) Expression of bcl-2.

H) Expression of Eomes. I) Expression of t-bet. J) Viral loads at day 5. Data from panels D-I are from DbGP276-specific CD8 T cells at day ~90 following LCMV Armstrong immunization. Gating scheme is shown on Fig. S3C. Acute infections were performed with LCMV Armstrong. Data are from 3 experiments, n=3-4 mice/group per experiment. *, P=0.05; **, P=0.02 (Mann-Whitney test). Error bars indicate SEM.

Fig. S13. Mechanism of immune dysregulation by CD4 T cell vaccines following chronic viral challenge. Preferential induction of CD4 T cell responses by CD4 T cell vaccines results in dysregulated expansion of memory CD4 T cells following chronic LCMV infection. Immune dysregulation is driven by persistent antigen, which results in uncontrolled expansion of memory CD4 T cells that override immune exhaustion and induce cytokine storm. Memory CD4 T cell dysregulation can be prevented by pre-exisiting CD8 T cell and antibody responses, which are able to control the infection. Most immune responses following infection of vaccination induce relatively greater CD8 T cell responses relative to CD4 T cell responses. This may represent an evolutionarily conserved mechanism, and altering this natural bias with CD4 T cell vaccines may result in a lethal outcome.

Table S1. Top genes enriched in CD4 T cells from LM-wt vaccination followed by LCMV Cl-13 challenge. Data are based on cDNA microarray analysis of Figure 4 and ordered by fold change (2nd column). Top 50 genes are included.

Table S2. Top genes enriched in CD4 T cells from LM-GP61 vaccination followed by LCMV Cl-13 challenge. Data are based on cDNA microarray analysis of Figure 4 and ordered by fold change (2nd column). Top 50 genes are included.

Table S3. Top gene sets enriched in CD4 T cells from LM-wt or LM-GP61 vaccination followed by LCMV Cl-13 challenge. Data are based on cDNA microarray analysis of Figure 4.

Fig S1

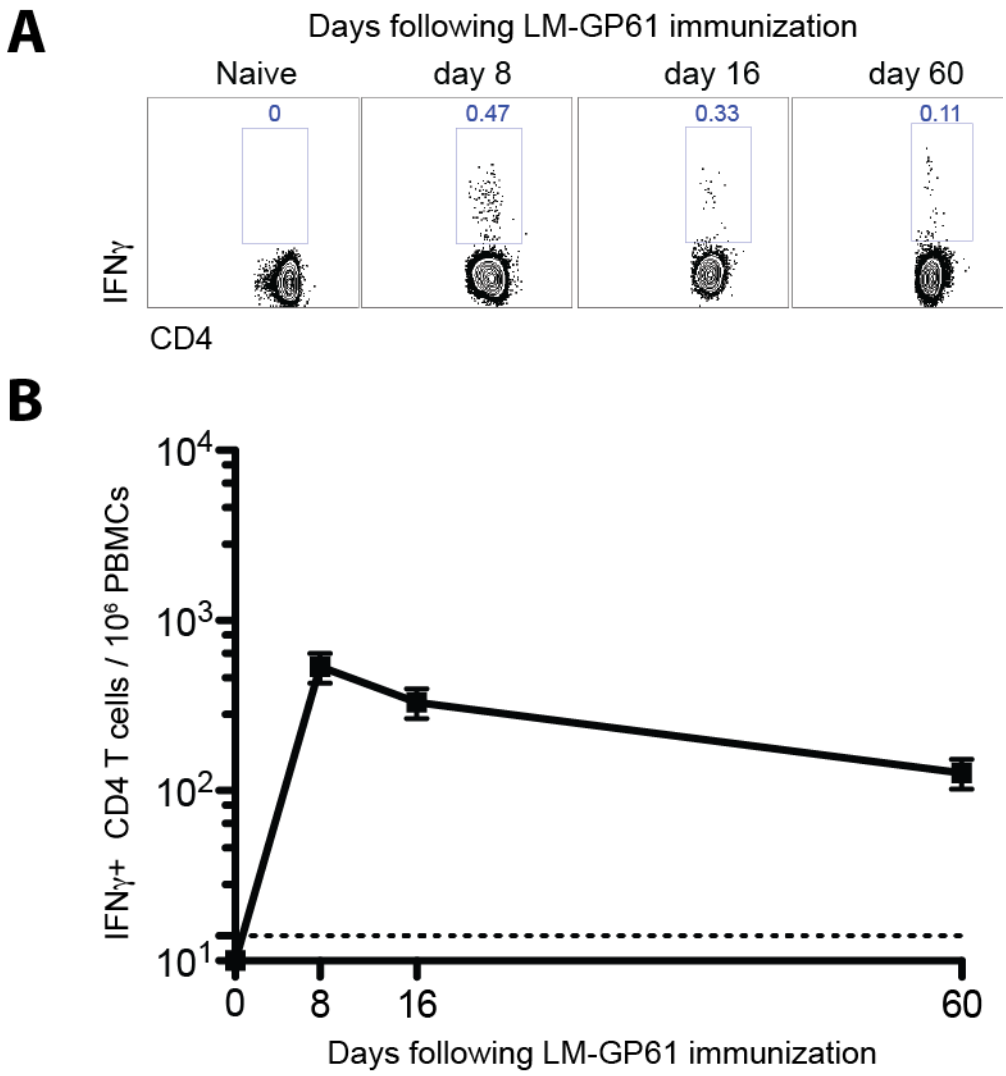
A
Days following LM-GP61 immunization
Naive
day 8
day 16
day 60
0
0.47
0.33
0.11
IFNγ
CD4
B
IFNγ+ CD4 T cells / 10⁶ PBMCs
10⁴
10³
10²
10¹
0
8
16
60
Days following LM-GP61 immunization

Fig S2

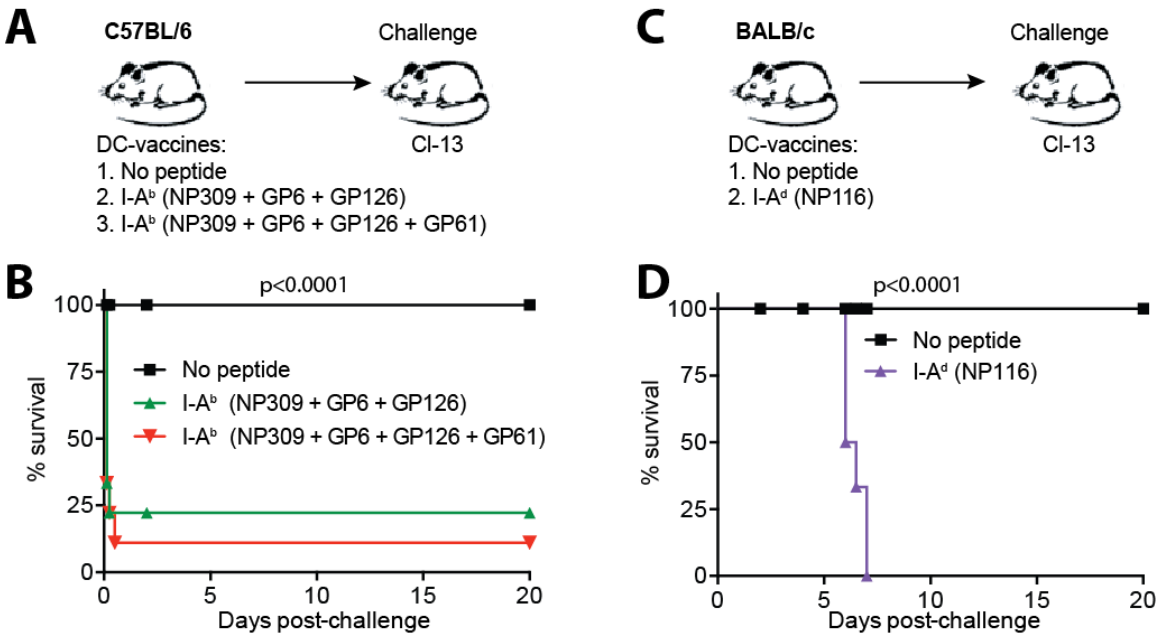
A
C57BL/6
Challenge
DC-vaccines:
1. No peptide
2. I-Aᵇ (NP309 + GP6 + GP126)
3. I-Aᵇ (NP309 + GP6 + GP126 + GP61)
Cl-13
C
BALB/c
Challenge
DC-vaccines:
1. No peptide
2. I-Aᵈ (NP116)
Cl-13
B
p<0.0001
% survival
No peptide
I-Aᵇ (NP309 + GP6 + GP126)
I-Aᵇ (NP309 + GP6 + GP126 + GP61)
Days post-challenge
D
p<0.0001
% survival
No peptide
I-Aᵈ (NP116)
Days post-challenge

Fig S3

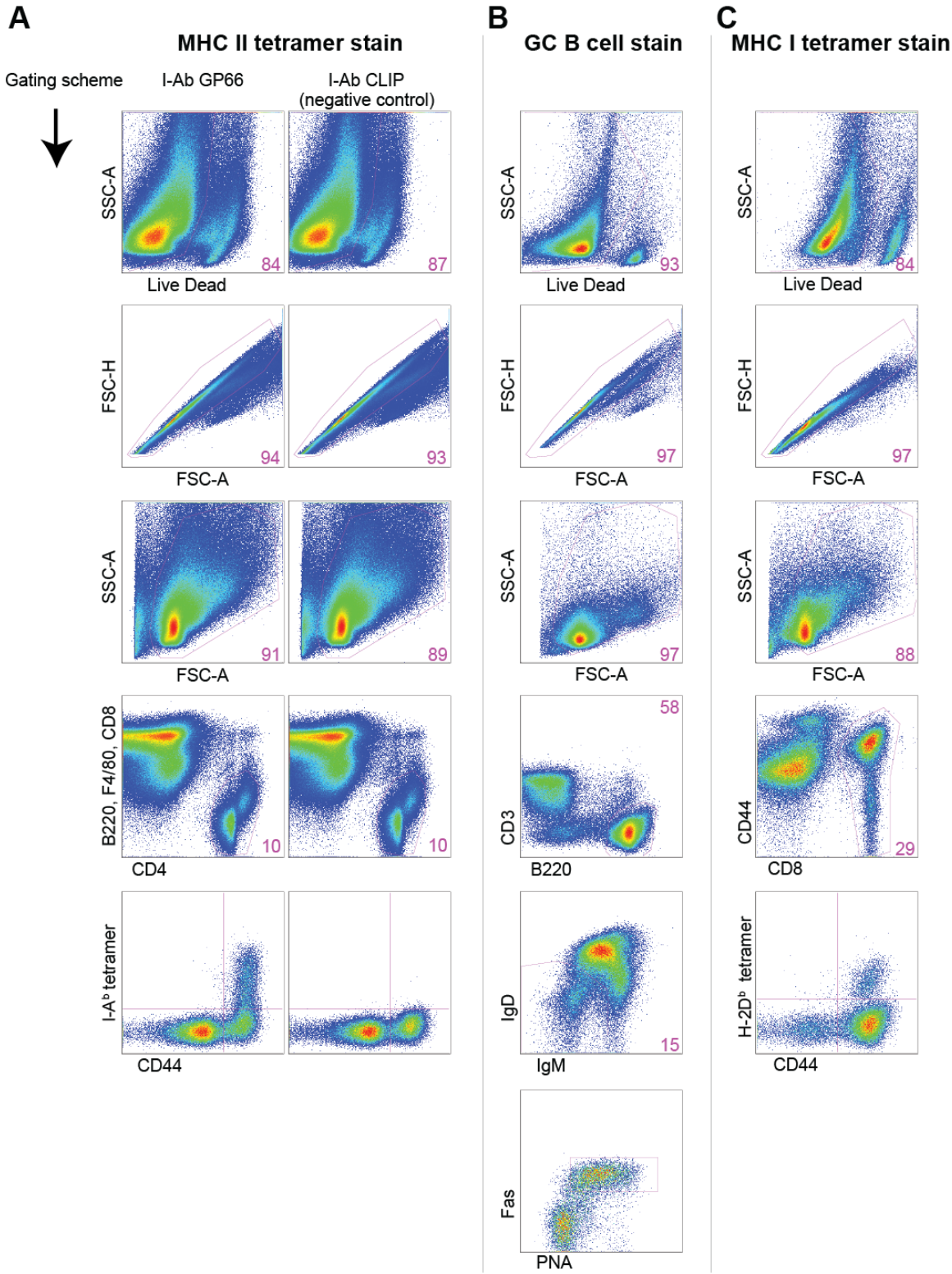
A
MHC II tetramer stain
Gating scheme
I-Ab GP66
I-Ab CLIP
(negative control)
SSC-A
Live Dead
84
87
FSC-H
FSC-A
94
93
SSC-A
FSC-A
91
89
B220, F4/80, CD8
CD4
10
10
I-Aᵇ tetramer
CD44
B
GC B cell stain
SSC-A
Live Dead
93
FSC-H
FSC-A
97
SSC-A
FSC-A
97
CD3
B220
58
IgD
IgM
15
Fas
PNA
C
MHC I tetramer stain
SSC-A
Live Dead
84
FSC-H
FSC-A
97
SSC-A
FSC-A
88
CD44
CD8
29
H-2Dᵇ tetramer
CD44

Fig S4

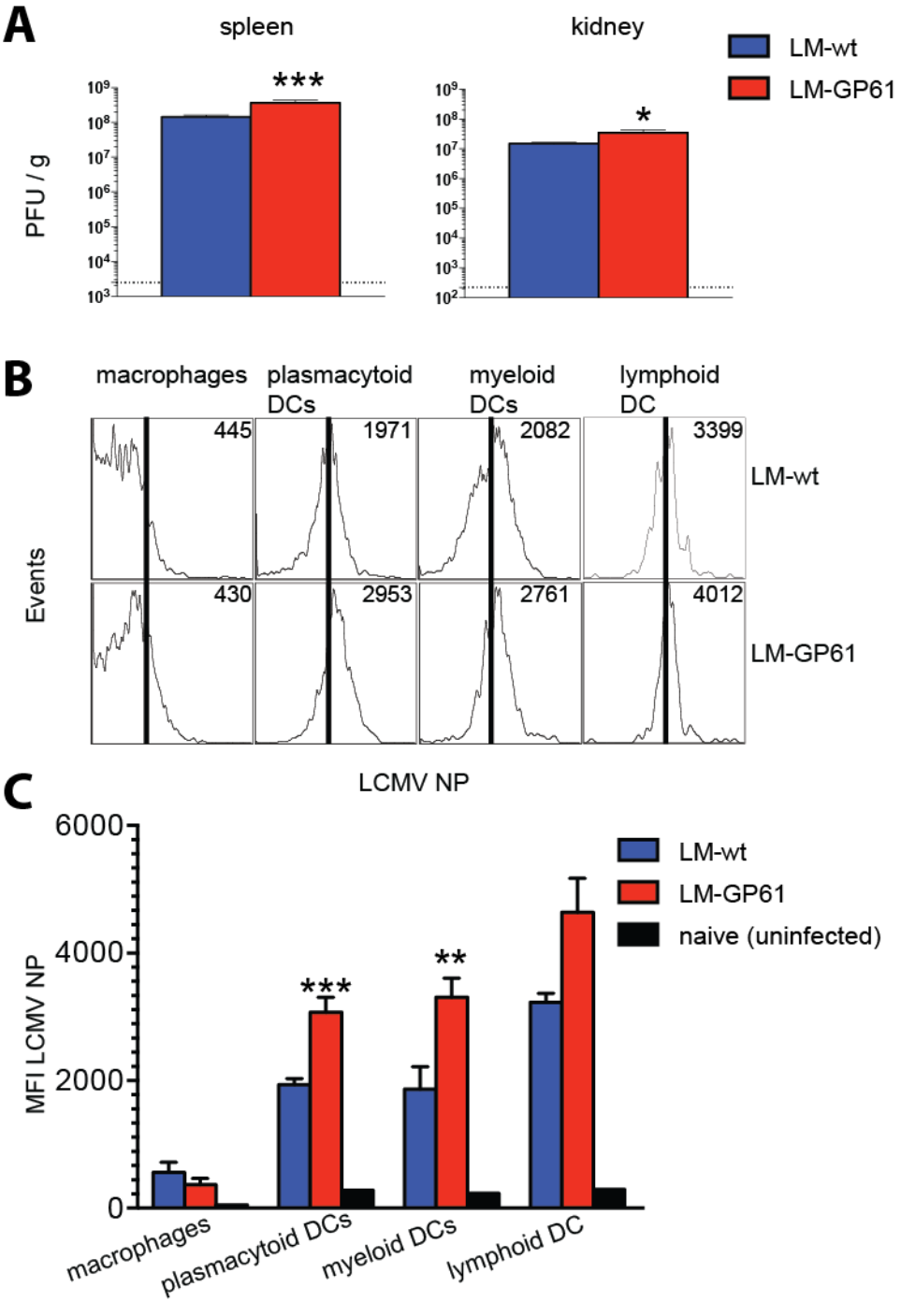
A
spleen
kidney
LM-wt
LM-GP61
PFU / g
***
*
B
macrophages
plasmacytoid DCs
myeloid DCs
lymphoid DC
445
1971
2082
3399
430
2953
2761
4012
LM-wt
LM-GP61
Events
LCMV NP
C
MFI LCMV NP
6000
4000
2000
0
LM-wt
LM-GP61
naive (uninfected)
***
**
macrophages
plasmacytoid DCs
myeloid DCs
lymphoid DC

Fig S5

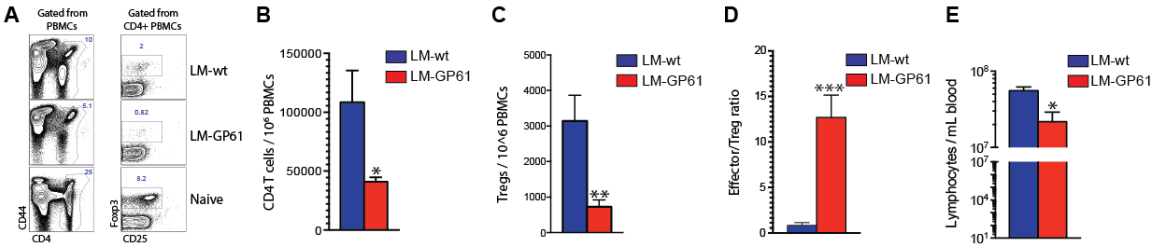
A
Gated from PBMCs
Gated from CD4+ PBMCs
LM-wt
LM-GP61
Naive
CD44
CD4
Foxp3
CD25
B
CD4 T cells / 10⁶ PBMCs
LM-wt
LM-GP61
C
Tregs / 10^6 PBMCs
LM-wt
LM-GP61
D
Effector/Treg ratio
LM-wt
LM-GP61
E
Lymphocytes / mL blood
LM-wt
LM-GP61

Fig. S6

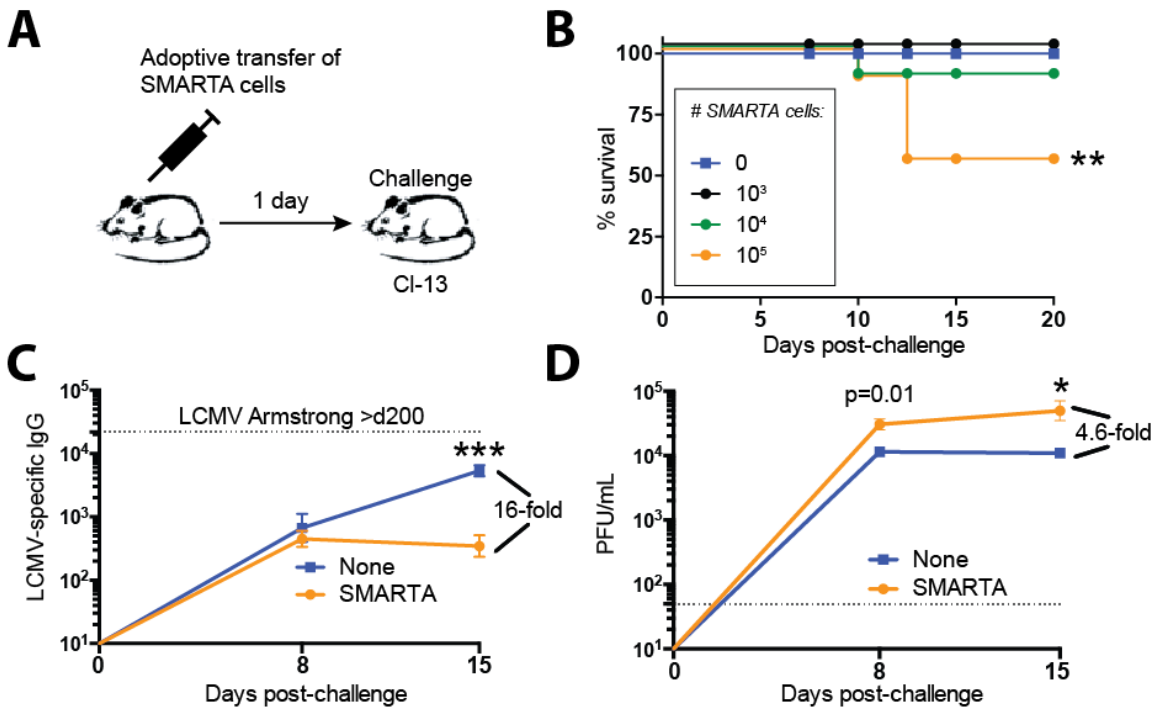
A
Adoptive transfer of SMARTA cells
1 day
Challenge
Cl-13
B
% survival
# SMARTA cells:
0
10³
10⁴
10⁵
**
Days post-challenge
C
LCMV-specific IgG
LCMV Armstrong >d200
***
16-fold
None
SMARTA
Days post-challenge
D
PFU/mL
p=0.01
*
4.6-fold
None
SMARTA
Days post-challenge

Fig. S7

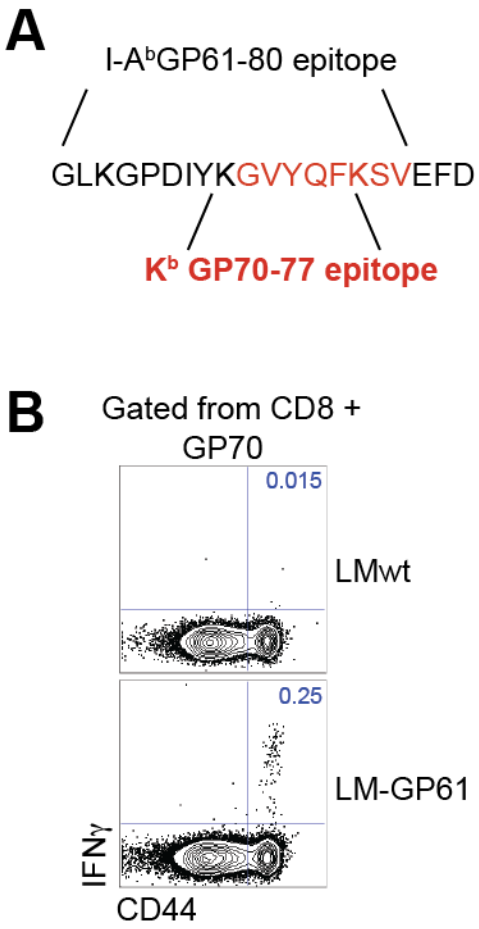
A
I-A^{b}GP61-80 epitope
GLKGPDIYKGVYQFKSVEFD
K^b GP70-77 epitope
B
Gated from CD8 +
GP70
0.015
LMwt
0.25
LM-GP61
IFNγ
CD44

Fig S8

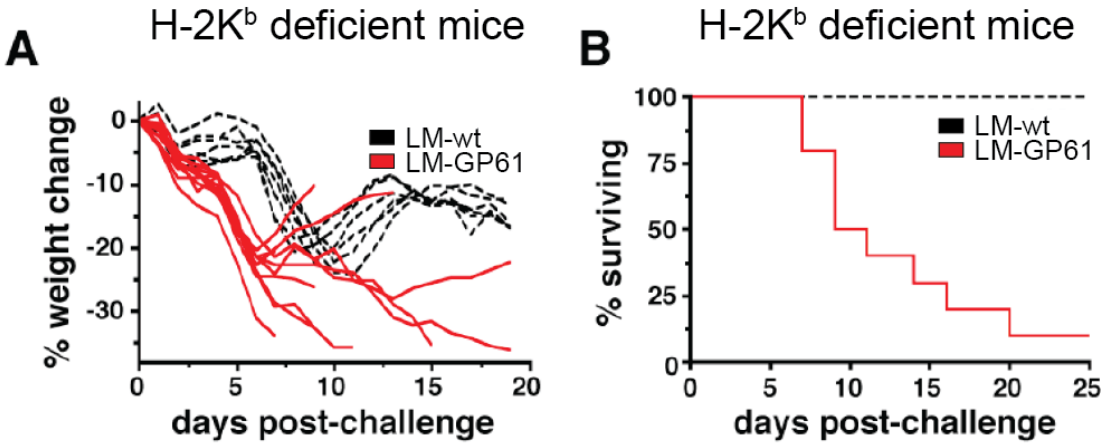
A
H-2K^b deficient mice
% weight change
0
-10
-20
-30
0
5
10
15
20
days post-challenge
LM-wt
LM-GP61
B
H-2K^b deficient mice
% surviving
100
75
50
25
0
0
5
10
15
20
25
days post-challenge
LM-wt
LM-GP61

Fig S9

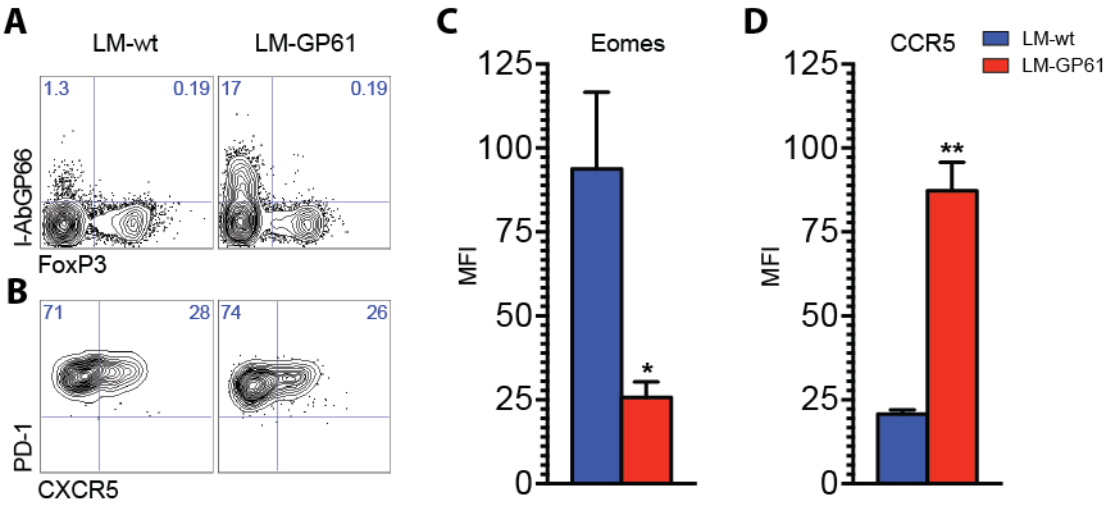
A
LM-wt
LM-GP61
1.3
0.19
17
0.19
I-AbGP66
FoxP3
B
71
28
74
26
PD-1
CXCR5
C
Eomes
MFI
125
100
75
50
25
0
*
D
CCR5
LM-wt
LM-GP61
MFI
125
100
75
50
25
0
**

Fig S10

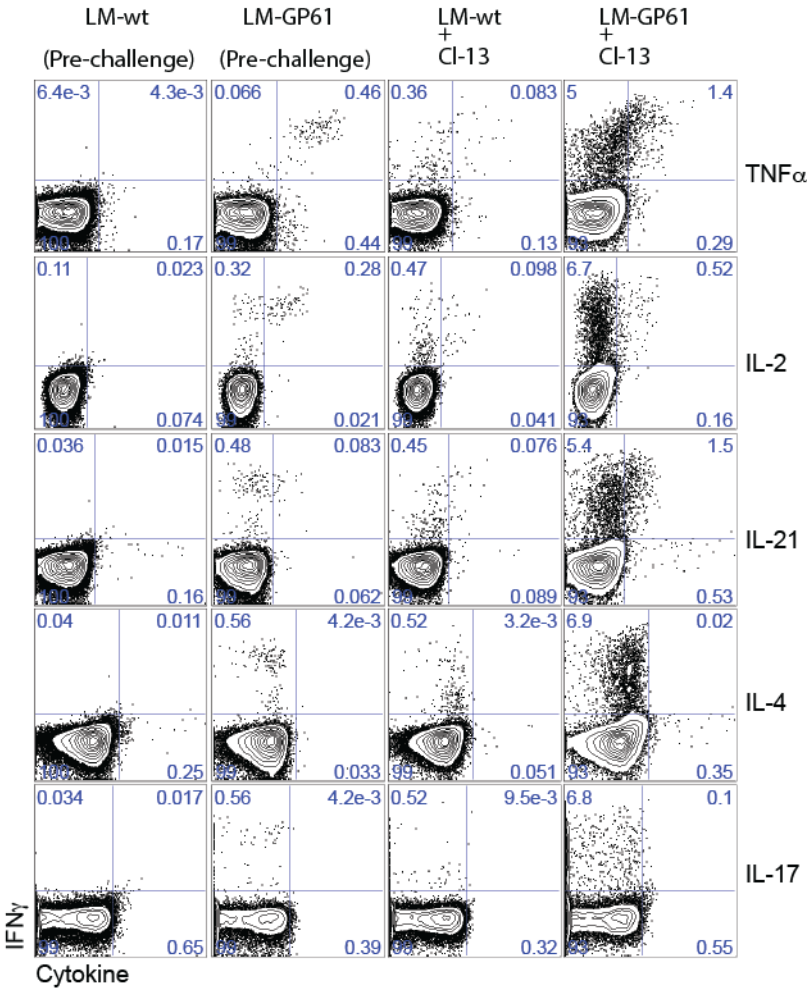
LM-wt
(Pre-challenge)
LM-GP61
(Pre-challenge)
LM-wt
+
Cl-13
LM-GP61
+
Cl-13
6.4e-3
4.3e-3
100
0.17
0.066
0.46
99
0.44
0.36
0.083
99
0.13
5
1.4
99
0.29
TNFα
0.11
0.023
100
0.074
0.32
0.28
99
0.021
0.47
0.098
99
0.041
6.7
0.52
99
0.16
IL-2
0.036
0.015
100
0.16
0.48
0.083
99
0.062
0.45
0.076
99
0.089
5.4
1.5
98
0.53
IL-21
0.04
0.011
100
0.25
0.56
4.2e-3
99
0.033
0.52
3.2e-3
99
0.051
6.9
0.02
99
0.35
IL-4
0.034
0.017
99
0.65
0.56
4.2e-3
99
0.39
0.52
9.5e-3
99
0.32
6.8
0.1
99
0.55
IL-17
IFNγ
Cytokine

Fig S11

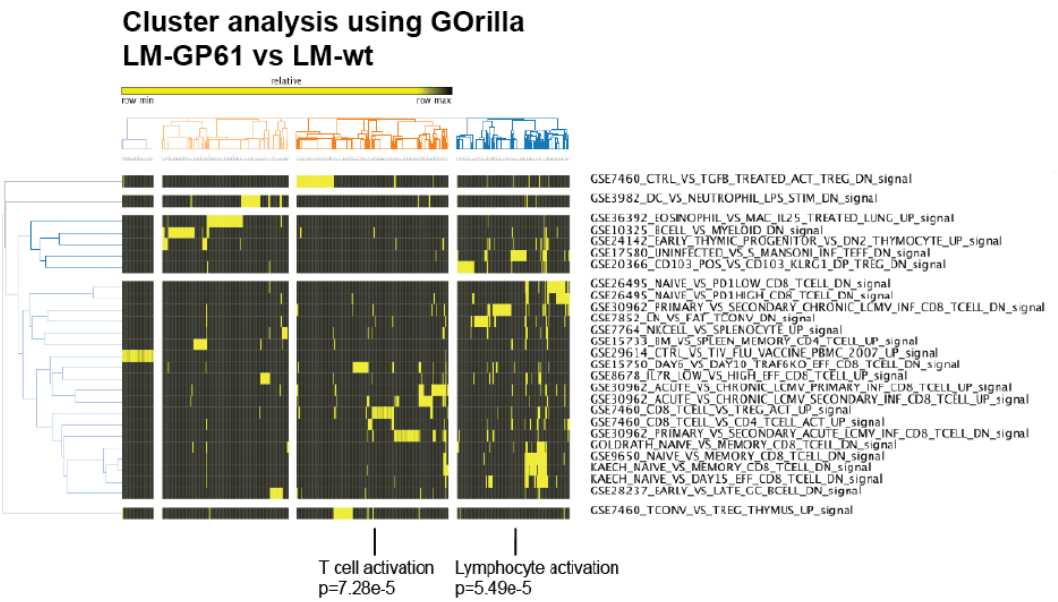
Cluster analysis using GOrilla
LM-GP61 vs LM-wt
relative
row min
row max
GSE7460_CTRL_VS_TGFB_TREATED_ACT_TREG_DN_signal
GSE3982_DC_VS_NEUTROPHIL_LPS_STIM_DN_signal
GSE36392_EOSINOPHIL_VS_MAC_IL25_TREATED_LUNG_UP_signal
GSE10325_BCELL_VS_MYELOID_DN_signal
GSE24142_EARLY_THYMIC_PROGENITOR_VS_DN2_THYMOCYTE_UP_signal
GSE17580_UNINFECTED_VS_S_MANSONI_INF_TEFF_DN_signal
GSE20366_CD103_POS_VS_CD103_KLRG1_DP_TREG_DN_signal
GSE26495_NAIVE_VS_PD1LOW_CD8_TCELL_DN_signal
GSE26495_NAIVE_VS_PD1HIGH_CD8_TCELL_DN_signal
GSE30962_PRIMARY_VS_SECONDARY_CHRONIC_LCMV_INF_CD8_TCELL_DN_signal
GSE7852_DN_VS_FAT_TCONV_DN_signal
GSE7764_NKCELL_VS_SPLENOCYTE_UP_signal
GSE15733_BM_VS_SPLEEN_MEMORY_CD4_TCELL_UP_signal
GSE29614_CTRL_VS_TIV_FLU_VACCINE_PBMC_2007_UP_signal
GSE15750_DAY5_VS_DAY10_TRAF6KO_EFF_CD8_TCELL_DN_signal
GSE8678_ITR_LOW_VS_HIGH_EFF_CD8_TCELL_UP_signal
GSE30962_ACUTE_VS_CHRONIC_LCMV_PRIMARY_INF_CD8_TCELL_UP_signal
GSE30962_ACUTE_VS_CHRONIC_LCMV_SECONDARY_INF_CD8_TCELL_UP_signal
GSE7460_CD8_TCELL_VS_TREG_ACT_UP_signal
GSE7460_CD8_TCELL_VS_CD4_TCELL_ACT_UP_signal
GSE30962_PRIMARY_VS_SECONDARY_ACUTE_LCMV_INF_CD8_TCELL_DN_signal
GOLDRATH_NAIVE_VS_MEMORY_CD8_TCELL_DN_signal
GSE9650_NAIVE_VS_MEMORY_CD8_TCELL_DN_signal
KAECH_NAIVE_VS_MEMORY_CD8_TCELL_DN_signal
KAECH_NAIVE_VS_DAY15_EFF_CD8_TCELL_DN_signal
GSE28237_EARLY_VS_LATE_GC_BCELL_DN_signal
GSE7460_TCONV_VS_TREG_THYMUS_UP_signal
T cell activation
p=7.28e-5
Lymphocyte activation
p=5.49e-5

Fig S12

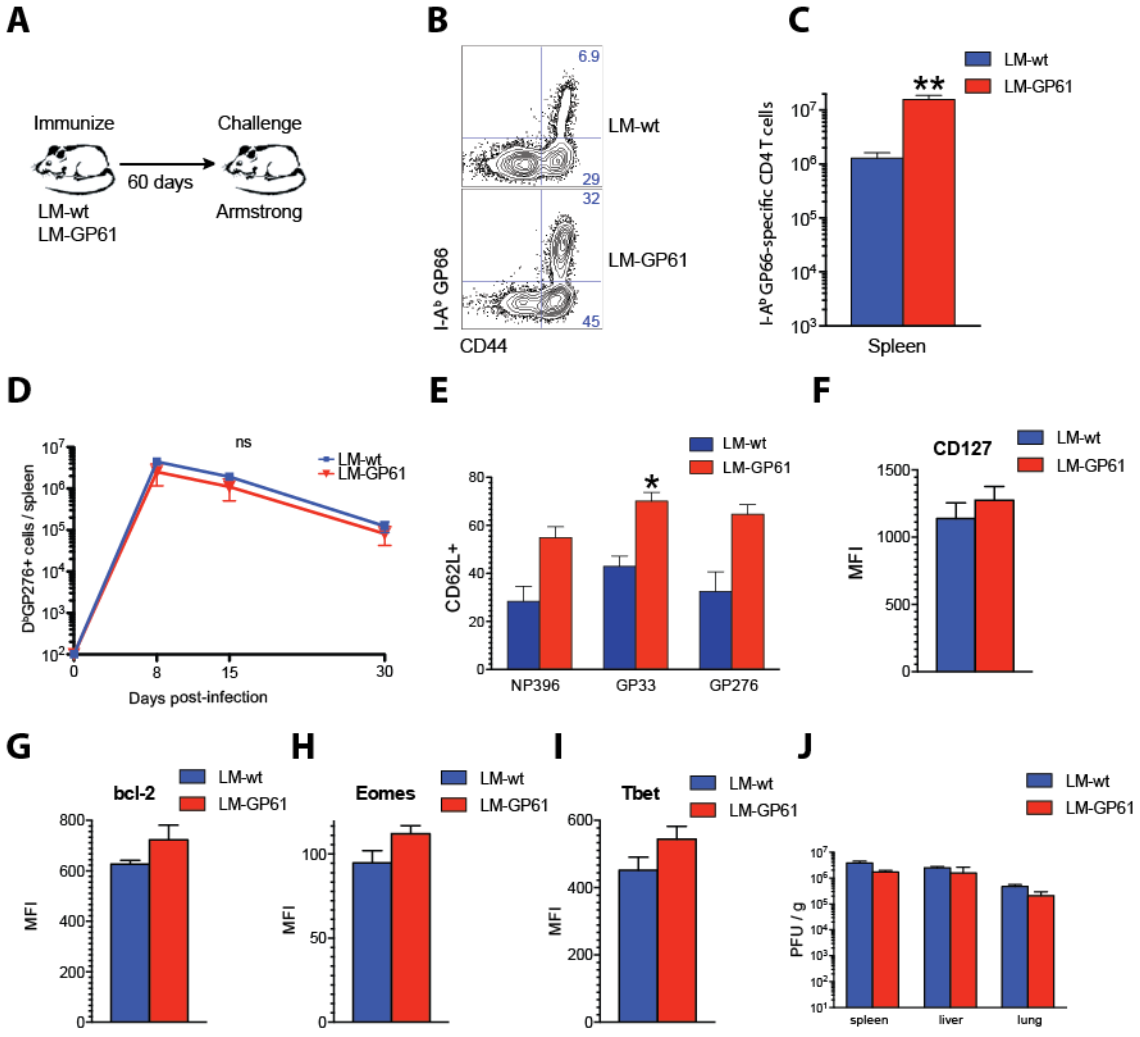
A
Immunize
Challenge
60 days
LM-wt
LM-GP61
Armstrong
B
6.9
29
32
45
LM-wt
LM-GP61
I-Aᵇ GP66
CD44
C
LM-wt
LM-GP61
**
I-Aᵇ GP66-specific CD4 T cells
Spleen
D
ns
LM-wt
LM-GP61
DᵇGP276+ cells / spleen
Days post-infection
E
LM-wt
LM-GP61
*
CD62L+
NP396
GP33
GP276
F
CD127
LM-wt
LM-GP61
MFI
G
bcl-2
LM-wt
LM-GP61
MFI
H
Eomes
LM-wt
LM-GP61
MFI
I
Tbet
LM-wt
LM-GP61
MFI
J
LM-wt
LM-GP61
PFU / g
spleen
liver
lung

Fig S13

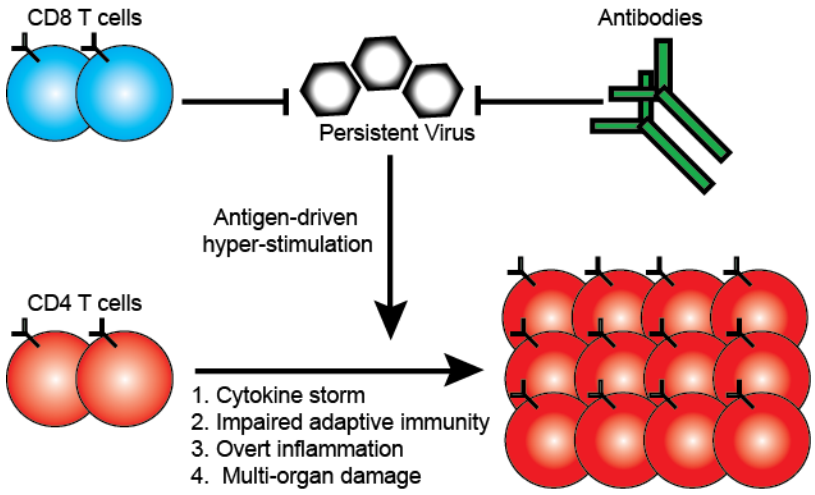
CD8 T cells
Antibodies
Persistent Virus
Antigen-driven
hyper-stimulation
CD4 T cells
1. Cytokine storm
2. Impaired adaptive immunity
3. Overt inflammation
4. Multi-organ damage

Table S1. Top 50 genes enriched in LM-wt v. LM-GP61 based on cDNA microarray analysis and ordered by fold change (2nd column)

Gene Symbol	Log 2 Fold Change	p-value (Asymptotic T test)
AURKB	5.6593	0.02787
IL22	5.6333	0.02997
HMGN3	5.6116	0.01466
2900062L11RIK	5.0725	0.02516
GCG	4.9031	0.04863
EOMES	4.6018	0.01837
PPIL5	4.3516	0.03335
SWAP70	4.2468	0.02405
SUSD2	4.1903	0.0581
KIT	4.1647	0.03044
ESCO2	4.1234	0.02593
MCM10	4.0432	0.02879
6430514L14RIK	4.0289	0.03922
PRR11	3.8208	0.02608
LAD1	3.7912	0.02273
CCNB2	3.7544	0.02175
A930038C07RIK	3.7071	0.388
PADI4	3.682	0.02705
DCTD	3.6525	0.3023
1700071A11RIK	3.6162	0.04653
SELL	3.5681	0.02308
2810433K01RIK	3.5546	0.03273
4932431H17RIK	3.552	0.02037
CCNF	3.4928	0.0391
UBE2C	3.4709	0.01996
KNTC1	3.3894	0.02904
H2-OB	3.3866	0.04693
NCAPG2	3.3855	0.03003
9230117N10RIK	3.3824	0.03131
MPZL1	3.3155	0.02893
DEPDC1A	3.3044	0.0401
LASS6	3.2826	0.02694
CEP55	3.2405	0.02325
PLXDC2	3.2279	0.03017
PBK	3.1467	0.02494
QSCN6L1	3.1413	0.0601
1110004B13RIK	3.1409	0.02644
RAD51AP1	3.1384	0.03054
MAN1C1	3.137	0.02485
E2F7	3.0862	0.03713
CDCA1	3.0671	0.0391
PRKRA	3.0666	0.5928
ADSSL1	3.0382	0.0407
TPX2	3.0305	0.03622
BIRC5	3.0137	0.02475
PPIC	3.0051	0.01875
KIF15	3.0034	0.03028
RAD51	3.0001	0.02803
NOC3L	2.9973	0.05796
SESTD1	2.9905	0.02933

Table S2. Top 50 genes enriched in LM-GP61 v. LM-wt based on cDNA microarray analysis and ordered by fold change (2nd column)

Gene Symbol	Log 2 Fold Change	p-value (Asymptotic T test)
KLRK1	9.2136	0.06493
SERPINA3G	6.2471	0.06544
KLRG1	4.9179	0.04649
BC005685	4.6354	0.05566
AA467197	4.384	0.03992
ARL4C	4.3164	0.04052
KCNJ8	4.3062	0.07663
KLRB1D	4.0819	0.06764
6230424C14RIK	4.0322	0.08232
SSBP2	3.8675	0.07541
ITGA1	3.8024	0.06788
CCR5	3.6658	0.04267
IGHG	3.5295	0.07094
IGK-V21-12	3.4954	0.05085
CTLA2B	3.3735	0.03877
CTLA2A	3.3436	0.03856
8430420C20RIK	3.2985	0.06516
LOC552908	3.2666	0.09544
A230057G18RIK	3.2424	0.04357
CLEC2G	3.1842	0.08974
EPHA3	3.1794	0.09531
CTLA2A	3.1736	0.03439
6720427H10RIK	3.1134	0.04914
RASD2	3.1107	0.06215
GZMF	3.0713	0.05845
9030208C03RIK	3.0441	0.03881
YES1	3.0327	0.06449
AW146020	3.0113	0.04268
DSP	2.9541	0.0756
CSF1	2.9266	0.05058
C030002C11RIK	2.8996	0.05656
1700012B18RIK	2.8813	0.0506
2610035D17RIK	2.876	0.06514
LOC641050	2.8533	0.04783
TMIE	2.8468	0.07089
2610507N02RIK	2.8183	0.05439
RGS1	2.8158	0.03293
LRRK1	2.8038	0.05277
KLRB1B	2.7946	0.04274
E230029C05RIK	2.7414	0.1057
CSPRS	2.739	0.04617
FGL2	2.6891	0.08082
AGRIN	2.6849	0.03109
TUBB4	2.6816	0.05345
AI120166	2.6263	0.078
2210408F21RIK	2.5989	0.06247
ADRB1	2.5723	0.06929
D12ERTD553E	2.5649	0.04997
KCTD12	2.5633	0.05962
C130090I23RIK	2.5588	0.08806

Table S3. Top gene sets enriched in CD4 T cells from LM-wt or LM-GP61 vaccination followed by LCMV Cl-13 challenge. Data are based on cDNA microarray analysis of Figure 4.

C7 gene set enriched in LM-GP61 v. LM-wt		
NAME	**NES**	**P value**
GSE30962_PRIMARY_VS_SECONDARY_CHRONIC_LCMV_INF_CD8_TCELL_DN	-2.4689	0.0000
GSE30962_PRIMARY_VS_SECONDARY_ACUTE_LCMV_INF_CD8_TCELL_DN	-2.2381	0.0000
GSE30962_ACUTE_VS_CHRONIC_LCMV_PRIMARY_INF_CD8_TCELL_UP	-2.0530	0.0000
GSE15750_DAY6_VS_DAY10_TRAF6KO_EFF_CD8_TCELL_DN	-2.0507	0.0000
GSE9650_NAIVE_VS_MEMORY_CD8_TCELL_DN	-1.7805	0.0000
GOLDRATH_NAIVE_VS_MEMORY_CD8_TCELL_DN	-1.7564	0.0000
KAECH_NAIVE_VS_MEMORY_CD8_TCELL_DN	-1.7500	0.0000
GSE7460_CD8_TCELL_VS_TREG_ACT_UP	-1.7491	0.0000
GSE7852_LN_VS_FAT_TCONV_DN	-1.7366	0.0000
GSE7460_CD8_TCELL_VS_CD4_TCELL_ACT_UP	-1.6817	0.0000
GSE29614_CTRL_VS_TIV_FLU_VACCINE_PBMC_2007_UP	-1.6772	0.0000
GSE10325_BCELL_VS_MYELOID_DN	-1.6592	0.0000
GSE26495_NAIVE_VS_PD1LOW_CD8_TCELL_DN	-1.6065	0.0024
GSE30962_ACUTE_VS_CHRONIC_LCMV_SECONDARY_INF_CD8_TCELL_UP	-1.5835	0.0045
GSE24142_EARLY_THYMIC_PROGENITOR_VS_DN2_THYMOCYTE_UP	-1.5702	0.0000
GSE17580_UNINFECTED_VS_S_MANSONI_INF_TEFF_DN	-1.5669	0.0000
GSE7764_NKCELL_VS_SPLENOCYTE_UP	-1.5227	0.0000
GSE8678_IL7R_LOW_VS_HIGH_EFF_CD8_TCELL_UP	-1.5163	0.0022
GSE26495_NAIVE_VS_PD1HIGH_CD8_TCELL_DN	-1.5161	0.0000
KAECH_NAIVE_VS_DAY15_EFF_CD8_TCELL_DN	-1.5095	0.0024
GSE15733_BM_VS_SPLEEN_MEMORY_CD4_TCELL_UP	-1.4996	0.0048
GSE3982_DC_VS_NEUTROPHIL_LPS_STIM_DN	-1.4949	0.0042
GSE7460_CTRL_VS_TGFB_TREATED_ACT_TREG_DN	-1.4914	0.0048
GSE36392_EOSINOPHIL_VS_MAC_IL25_TREATED_LUNG_UP	-1.4913	0.0071
GSE20366_CD103_POS_VS_CD103_KLRG1_DP_TREG_DN	-1.4891	0.0046
GSE28237_EARLY_VS_LATE_GC_BCELL_DN	-1.4430	0.0049
GSE7460_TCONV_VS_TREG_THYMUS_UP	-1.4099	0.0092